High Expression of SAMM50 Indicates Poor Clinical Prognosis in Hepatocellular Carcinoma and Represents a Potential Novel Biomarker

Huawei Zhai
Banglian Cai
Zihao Zheng
Fujing Cai
Zhenmiao Wan
Yuchen Pan
Guangzheng Sun
Haifeng Zhang
Jinhai Li
lijindahai@126.com

Research Article

Keywords: SAMM50, HCC, immunohistochemistry, survival, independent prognostic factor

Posted Date: May 13th, 2026

DOI: https://doi.org/10.21203/rs.3.rs-9536726/v1

Additional Declarations: No competing interests reported.

Abstract

Background

Identifying diagnostic and prognostic biomarkers and therapeutic targets for hepatocellular carcinoma (HCC) is essential to improve risk stratification, guide individualized treatment, and enhance therapeutic efficacy.

Methods

The expression of SAMM50 was initially analyzed in publicly accessible curated genomic and proteomic databases, such as the Cancer Cell Line Encyclopedia, the Human Protein Atlas, and other HCC-specific repositories. This analysis revealed differential expression patterns between HCC and non-neoplastic liver tissue. Subsequently, clinicopathological data and tissue specimens were collected from 200 HCC patients who underwent treatment at our institution. The protein and transcript levels of SAMM50 were experimentally measured in paired HCC and adjacent non-tumorous tissues using immunohistochemistry (IHC) and quantitative reverse transcription polymerase chain reaction (qRT-PCR). The association between SAMM50 expression and key clinicopathological features was further evaluated. Univariate and multivariate Cox proportional hazards analyses were performed to determine the independent prognostic value of SAMM50 expression in HCC. Based on these results, a reproducible and clinically applicable nomogram, supported by a forest plot, was constructed to facilitate prognostic prediction and support individualized therapeutic decision-making. Finally, in vitro and in vivo experiments were conducted to characterize the phenotypic alterations in HCC cells after SAMM50 knockdown, thereby confirming its involvement in critical oncogenic behaviors.

Results

This research demonstrated that the mRNA and protein levels of SAMM50 in HCC tissues were elevated compared to those in normal liver and adjacent tissues. Immunohistochemistry findings confirmed that SAMM50 protein levels were persistently higher in HCC tissues than in paired adjacent tissues. High expression of SAMM50 was correlated with unfavorable clinicopathological factors, encompassing pretreatment alpha-fetoprotein (AFP) levels, tumor size, T stage, American Joint Committee on Cancer (AJCC) stage, histological grade, and worse overall survival.Specifically, high expression of SAMM50 was linked to shorter overall survival (OS), progression-free survival (PFS), and disease-free survival (DFS). Moreover, univariate and multivariate Cox analyses were conducted to investigate the association between SAMM50 expression and clinicopathological features in HCC patients and to identify independent prognostic factors. The area under the receiver operating characteristic (ROC) curve (AUC) for SAMM50 was 0.863, indicating that it can function as a diagnostic marker for HCC. Silencing of SAMM50 inhibited HCC cell proliferation, migration, and invasion, promoted apoptosis in vitro, and suppressed HCC growth in vivo.

Conclusion

This research demonstrates that SAMM50 serves as a promising biomarker for the diagnosis and prognosis of HCC. The results of this study not only contribute to the evaluation of baseline data and risk stratification in HCC but also offer novel approaches for the development of precise treatment strategies and targeted therapies.

Introduction

Despite advances in systemic therapy, hepatocellular carcinoma (HCC) remains a prevalent malignancy worldwide. The postoperative recurrence rate of HCC ranges from 50% to 80%[1, 2]. One contributing factor to this high recurrence rate is the absence of specific biomarkers for accurate postoperative assessment. This shortcoming contributes significantly to the high mortality rate among HCC patients and underscores a crucial gap in the understanding and management of the disease[3, 4]. Biomarkers can facilitate the formulation of precise treatment strategies and enable accurate prognostic evaluations. Moreover, they are regarded as effective risk stratification tools for determining the optimal timing for the implementation of systemic therapy[5]. Therefore, the identification of sensitive and effective prognostic biomarkers is pivotal for enhancing the detection of clinically significant HCC cases and improving treatment efficacy.

SAMM50 plays a critical role in mitochondrial biology; it not only functions as a constituent of the mitochondrial complex that bridges the inner and outer mitochondrial membranes but also plays a key part in the sorting and assembly machinery (SAM) responsible for the assembly of β-barrel proteins in the outer membrane. The dual functionality of SAMM50 is indispensable for regulating mitochondrial morphology, particularly the structure of cristae[6]. Additionally, SAMM50 interacts with the mitochondrial contact site and cristae organizing system (MICOS) complex to form the MICOS-MIB-SAM (MBI) supercomplex, thereby facilitating the connection between the inner and outer mitochondrial membranes[7]. Notably, loss of SAMM50 leads to Pink1-Parkin-dependent mitochondrial autophagy and promotes mtDNA aggregation, safeguarding it from autophagic removal. Chen et al.[8] demonstrated that loss of SAMM50 in hepatocytes triggers mitochondrial membrane remodeling, resulting in mtDNA release and subsequent liver injury. Furthermore, recent studies have identified SAMM50 gene mutations that alter mitochondrial metabolism and contribute to malignant tumor progression. These findings highlight SAMM50's potential as a diagnostic and prognostic cancer biomarker[9–11].

Numerous investigations have indicated that SAMM50 variations play a significant role in the development and progression of non-alcoholic fatty liver disease and liver injury, which are gradually emerging as potential etiologies of HCC[12–15]. Although SAMM50 has been associated with precancerous HCC lesions, studies exploring its expression in HCC tissues, its correlation with clinicopathological factors, and its prognostic influence are scarce. Therefore, based on bioinformatic analyses, this study aims to analyze SAMM50 expression in tumor and non-tumor samples from 200

HCC patients, investigate the relationship between SAMM50 and clinicopathological factors, and evaluate SAMM50's role in predicting HCC prognosis. Finally, in vitro and in vivo experiments were conducted to validate the biological function of SAMM50 in HCC cells. The findings suggest that SAMM50 is a valuable biomarker for HCC diagnosis and prognosis assessment.

Materials and Methods

Bioinformatics assay

The expression of SAMM50 mRNA across different cancer types was analyzed using online TCGA datasets (http://ualcan.path.uab.edu/index.html). In addition, SAMM50 mRNA expression in different liver tissues was studied using the Hepatocellular Carcinoma Database (HCCDB,http://lifeome.net/database/hccdb). Simultaneously, co-expression networks in adjacent and HCC tissues were assessed via HCCDB. Data were normalized using log2 FC, and *p*-values were adjusted with the Benjamini-Hochberg correction. The UALCAN database was used to explore associations between SAMM50 mRNA expression and clinicopathological parameters.

The LinkedOmics database was used to identify positively and negatively co-expressed genes correlated with SAMM50. In addition, we performed Gene Ontology (GO) and Kyoto Encyclopedia of Genes and Genomes (KEGG) enrichment analyses on co-expressed genes in HCC and adjacent liver tissues. To further understand the mechanisms involving this gene, we used the STRING database to conduct a protein-protein interaction (PPI) network analysis. To gain a deeper understanding of which HCC cell lines exhibit higher SAMM50 expression, its suborganelle localization, and its protein expression profile in human HCC tissues, we conducted a search using the HPA database. The Kaplan-Meier Plotter (http://kmplot.com/analysis/index.php?p=service&cancer=liver_rnaseq) was applied to predict the relationship between SAMM50 expression and HCC patient prognosis.

Sample collection

A total of 200 pairs of HCC tissues and adjacent normal tissues (located ≥ 2 cm from the tumor tissue) were procured from HCC patients at the Third Affiliated Hospital of Wenzhou Medical University, China. This study was approved by the Research Ethics Committee (Approval No. : YJ2025120), and written informed consent was obtained from all participants. The sample size of 200 pairs was determined based on a power analysis assuming a two - sided significance level of 0.05 and a power of 80%, referencing previous HCC biomarker studies with similar design[16]. Given the retrospective nature of this study, no randomization was performed. All consecutive eligible HCC patients who underwent curative liver resection at our institution between January 2019 and December 2024 were enrolled according to the predefined inclusion and exclusion criteria. Immunohistochemical (IHC) analysis and quantitative reverse transcription polymerase chain reaction (qRT-PCR) were conducted to assess the expression of SAMM50 and its correlation with HCC. Postoperative pathology verified that all patients underwent R0

resection. The inclusion criteria were as follows: 1) absence of liver fibrosis or cirrhosis, as confirmed by preoperative liver stiffness measurement (LSM) using transient elastography (FibroScan, LSM < 7.0 kPa indicating no significant fibrosis) and further validated by postoperative histopathological examination of resected non-tumorous liver tissue (Ishak score ≤ 2 for fibrosis, no evidence of cirrhosis); 2) no prior history of radiotherapy, chemotherapy, targeted therapy, or immunotherapy before liver resection; 3) no prior history of liver surgery; 4) no prior history of other malignancies, diabetes, or autoimmune diseases. The exclusion criteria were as follows: (1) presence of extrahepatic metastasis or vascular invasion confirmed by preoperative imaging; (2) history of other malignancies within the past 5 years; (3) receipt of neoadjuvant therapy including radiotherapy, chemotherapy, targeted therapy, or immunotherapy prior to surgery; (4) severe organ dysfunction (heart, lung, kidney) that precluded surgical treatment; (5) incomplete clinical or follow-up data.

Cell lines

The hepatocellular carcinoma cell models MHCC-97H, HCC-LM3, HepG2, and Huh7, along with the non-malignant hepatic cell line LO2, were procured from the American Type Culture Collection. These relevant hepatic cell types were cultured in Dulbecco's Modified Eagle Medium sourced from Gibco in the United States. The culture medium was supplemented with 10% fetal bovine serum and a 1% antibiotic mixture. Cell proliferation was conducted in a controlled environment with 5% carbon dioxide at 37 ℃.

Immunohistochemical analysis

An immunohistochemical (IHC) assay kit (Bioengineering Co., Ltd, Shanghai, China) was employed in strict accordance with the manufacturer's guidelines. Specifically, rabbit anti-human SAMM50 antibody (Proteintech Group, Inc., Chicago, USA) was diluted and applied to each slide, ensuring complete coverage of the tissue specimens. Subsequently, the slides underwent incubation, dehydration, and air-drying processes prior to mounting. Positive staining for SAMM50 manifested as yellowish granules predominantly within the cytoplasm.

Two seasoned pathologists, blinded to patient-related data and experimental conditions, independently assessed the immunoreactive score (IRS). The IRS was computed by integrating the percentage of positively stained cells with the staining intensity. The staining intensity was graded as 0 (negative), 1 (weak), 2 (moderate), and 3 (strong), while the percentage of positively stained cells (immunoreactivity) was scored as 1 (0 ~ 25%), 2 (26 ~ 50%), 3 (51 ~ 75%), and 4 (76 ~ 100%)[17]. The expression level of SAMM50 was categorized as low (IRS: 0 ~ 6) or high (IRS: 8 ~ 12). The staining intensity and immunoreactivity were quantified based on the integrated optical density (IOD) measured using the Image-Pro Plus 6.0 software.

RNA extraction

Total ribonucleic acid (RNA) was isolated from tissue specimens employing the TRIzol reagent (Fusheng Industrial Co., Ltd., Shanghai, China) in accordance with the manufacturer's guidelines. A total of 1 microgram of the extracted RNA was employed to synthesize complementary deoxyribonucleic acid (cDNA) using a reverse transcriptase reaction kit (Beijing Fubo Biotechnology Co., Ltd.).

Quantitative reverse transcription polymerase chain reaction

Quantitative polymerase chain reaction (qPCR) was performed on the Biorad CFX 96 Touch platform using SYBR Green Supermix (a fluorescent stain specific to double-stranded DNA) (Zhongshan Golden Bridge Biotechnology Co., Ltd, Beijing, China). The mRNA expression of target genes was normalized to that of GAPDH. The primers used for amplification were designed and synthesized by Shanghai Kaiji Gene Technology Joint Stock Co., Ltd. The specific primer sequences are as follows: SAMM50 forward, 5'-GGTCGCTTTAGCCTTAG-3'; SAMM50 reverse, 5'-TAACTTTAGGAATAGCAT-3'; GAPDH forward, 5'-CGCAGAGACCTCAACTACATATCGTAC-3'; GAPDH reverse, 5'-TCACGCGCAGTCCGTAGCA-3'. The relative mRNA expression of SAMM50 was calculated using the $2^{-\Delta\Delta Ct}$ method according to the manufacturer's instructions.

Follow-up

Postoperatively, patients underwent regular follow-up, with a minimum of one follow-up session every three months, via outpatient consultations, telephone inquiries, or home visits. During the follow-up, overall survival (OS), progression-free survival (PFS), and disease-free survival (DFS) were evaluated to monitor the long-term recovery and health status of patients.

Nomogram evaluation

Calibration curves were constructed by plotting the predicted survival probabilities derived from the nomogram against the actual outcomes. The existence of a 45° line signified superior predictive performance of the nomogram. Moreover, the discriminatory performance of the nomogram was assessed using the concordance index (C-index), and its predictive accuracy was compared with that of individual prognostic factors through both the C-index and receiver operating characteristic (ROC) curves. The pROC package was employed for ROC analysis. An area under the ROC curve (AUC) value ranging from 0.5 to 1.0 indicated a discrimination capacity of 50 ~ 100%.

Western blot

Total cellular protein was extracted from hepatocellular carcinoma (HCC) cells using RIPA lysis buffer (Beyotime, China). Protein quantification was carried out through the utilization of a bicinchoninic acid assay kit (Beyotime). Subsequently, Western blot analysis was conducted in accordance with

established protocols[18]. Specifically, proteins were separated via SDS-polyacrylamide gel electrophoresis and then electrophoretically transferred onto nitrocellulose membranes. After blocking with non-fat milk, the membranes were incubated successively with specific primary antibodies and corresponding horseradish peroxidase-conjugated secondary antibodies. Immunoreactive bands were visualized by means of an enhanced chemiluminescence detection system (Thermo Fisher Scientific). The primary antibody against SAMM50 (orb221929, Biorbyt Ltd) was employed at a dilution ratio of 1:1000.

Cell EdU,proliferation, scratch, invasion, migration and apoptosis analysis

Cellular proliferation ability was assessed in accordance with established protocols[19]. In the CCK-8 assay, cells transfected with specific small interfering RNA (siRNA) were inoculated into 96-well plates at an initial density of 1.5×10^3 cells per well. After incubation for specified time intervals, the proliferative activity was quantitatively analyzed using a Cell Counting Kit-8. Regarding the colony formation assay, 500 siRNA-transfected cells were seeded per well in 6-well plates and cultivated for 10 days. The resultant cell colonies were fixed, stained with a 0.1% (weight/volume) crystal violet solution, and manually enumerated. For the EdU assay, cells transfected with specific siRNA were incubated with 10 μM EdU for 2 hours, followed by fixation, permeabilization, and click reaction with Apollo® fluorescent dye to label proliferating cells according to the manufacturer's instructions.Moreover, the influence of SAMM50 knockdown on the invasiveness, migratory capacity, and apoptotic rate of tumor cells was investigated based on previous methodology[20].

Mouse model

All animal-related procedures obtained prior approval from the Institutional Animal Care and Use Committee of Wenzhou Medical University (Ethical Approval Number: RY202508074) and were carried out in accordance with a previously reported protocol[21]. Specifically, female BALB/c nude mice aged between 3 and 4 weeks were randomly allocated into three experimental groups, with five mice in each group. Subsequently, a suspension containing 5×10^6 Huh7 cells, either with stable SAMM50 knockdown or control cells, was subcutaneously injected into the right axillary region of each mouse. Tumor growth was monitored by measuring the dimensions using a caliper at three-day intervals. Tumor volumes were calculated according to the formula: Volume = (longest diameter × shortest diameter^2) / 2.

Statistical analysis

GO and KEGG enrichment analyses were carried out utilizing the "ggplot2" (v3.3.3) and "clusterProfiler" (v3.15.3) packages in R. Terms with an adjusted p - value (p.adj) less than or equal to 0.05 were regarded as statistically significant. The associations between SAMM50 expression levels and clinicopathological parameters in patients with HCC were evaluated using either Pearson's chi-square test or Fisher's exact test, as applicable. Overall survival (OS) was estimated via the Kaplan – Meier method, and the differences between groups were compared by means of the log - rank test. Independent prognostic

factors for postoperative HCC outcomes were identified through Cox proportional hazards regression analysis. Receiver operating characteristic (ROC) curve analysis was conducted in GraphPad Prism to assess diagnostic accuracy, with the area under the curve (AUC), its 95% confidence interval (95% *CI*), sensitivity, and specificity being reported. All statistical computations were performed using SPSS (version 18.0) and GraphPad Prism (version 8.0) software. All p - values were obtained from two - sided tests, and statistical significance was defined as $^{*}p < 0.05$, $^{**}p < 0.01$, and $^{***}p < 0.001$.

Results

mRNA and Protein Expression of SAMM50 in Different Databases

Analysis of TCGA data revealed that SAMM50 undergoes frequent genomic alterations across multiple cancer types, with an amplification rate > 0.5% and a deletion rate > 0.2% in HCC cases (Supplementary Figure S1A). To further characterize its potential role in HCC pathogenesis, we conducted comprehensive expression analyses using TCGA and CPTAC cohorts via online bioinformatics platforms (http://ualcan.path.uab.edu/index.html). The results indicated consistent SAMM50 upregulation in HCC at both the mRNA and protein levels ($P < 0.001$, Figs. 1A-B). In addition, we investigated differential SAMM50 mRNA expression levels in HCC cells, HCC tissues, and normal tissues using MERAV. The results demonstrated consistent SAMM50 upregulation in HCC at the mRNA level ($P < 0.01$ or $P < 0.001$, Fig. 1C). Stage-specific analysis revealed more pronounced SAMM50 expression in advanced-stage HCC patients compared to early-stage cases (Fig. 1D). Next, we examined HCCDB to determine whether there were significant differences in SAMM50 mRNA expression levels across HCC datasets. SAMM50 levels in HCC tissues were higher than in adjacent tissues (HCC/adjacent: logFC = 0.50) (Fig. 1E). Subsequently, in the HCCBD dataset (Supplementary Figure S1B), scaled SAMM50 expression was detected in four different liver states: healthy, cirrhotic, adjacent, and HCC. The results showed that SAMM50 expression was most tightly clustered and lowest in the healthy state. In the CRISPR screening data, 783 out of 1186 cell lines were classified as "Common Essential" (genes that are widely essential). Meanwhile, in the RNAi screening data, 206 out of 343 cell lines were classified as "Strongly Selective" (genes with high selectivity). The peak values of the distribution curves for both datasets were concentrated in the Gene Effect range of -0.5 to 0.0 and showed a right-skewed distribution. This indicates that SAMM50 has a significant dependency effect in most cell lines (Supplementary Figure S1C). The gene function screening results indicate that SAMM50 is a potentially broadly essential or highly selective gene target, warranting further study regarding its value in maintaining cellular functions and as a therapeutic target.

GO and KEGG analyses of SAMM50 and its co-expressed genes in HCC.

To better understand the biological role of SAMM50, the Linked Omics database was used to identify co-expressed genes that are both positively and negatively correlated with SAMM50 (Fig. 2A). Heat maps were used to visualize the 50 genes most strongly correlated with SAMM50 (Figs. 2B, C). Next, using the

HCCDB, we analyzed the co-expression networks of SAMM50 and found significant differences between HCC tissues and adjacent liver tissues (Figs. 2D, E). In addition, we performed GO enrichment analysis of the co-expressed genes in HCC tissues and adjacent liver tissues. The results suggest that the SAMM50 gene collection is significantly enriched in mitochondrial membrane-related functions, especially in the process of protein localization and insertion into the mitochondrial membrane, as well as the formation of mitochondrial outer membrane protein complexes. This indicates that these genes may be involved in key biological processes such as mitochondrial biogenesis, protein transport, or maintenance of mitochondrial membrane structure. (Fig. 2F). GSEA revealed notable differences in the enrichment direction and intensity of SAMM50 across samples. For example, it is significantly activated in some samples of the interferon-related pathway, whereas it is inhibited in some samples of the ribosome pathway(Supplementary Figure S2).

The establishment of the "PPI network" of the SAMM50 protein and its localization in the cell.

To further understand the mechanisms of this gene, we used the STRING database to analyze protein-protein interactions and identified the strongest interactions with TOMM40, TOMM22, IMMT, MTX3, MICOS10, and MTX1 (Fig. 3A). This network diagram reveals the core components of the mitochondrial protein input system, where these proteins work together to ensure that nuclear-encoded mitochondrial proteins can be accurately transported to different compartments of the mitochondria, which is crucial for maintaining mitochondrial function and cellular energy metabolism. The HPA database showed that the SAMM50 protein in human cells, SAMM50 was mainly located in vesicles and the Golgi apparatus, as shown by immunofluorescence experiments (Fig. 3B), and it was moderately expressed in HCC tissues by IHC, localized primarily in the cytoplasm (Fig. 3C).

To explore the association between SAMM50 level and OS (Overall Survival) in HCC patients, we used the Kaplan-Meier plotter tool and found a significant correlation between high expression of SAMM50 and poor prognosis (Fig. 3D, P = 0.012). Furthermore, based on the TCGA dataset, we conducted ROC analysis using the pROC package and calculated the AUC to be 0.898 (Supplementary Figure S3).

Analysis of the Relationship between SAMM50 expression and the clinicopathological characteristics of HCC patients

Paired tumor and adjacent standard tissue samples were obtained from 200 patients with HCC who underwent routine liver resection, which included anatomical and non-anatomical resections. Pathological examination revealed the absence of cancer cells in adjacent tissues. Of the 200 patients, 99 (49.5%) had poorly differentiated tumors, 143 (71.5%) tested positive for HBsAg, 11 (5.5%) had lymph node metastasis, and 118 (59%) underwent anatomical resection. Tumor staging was based on the eighth edition of the AJCC staging system, with 102 (51.0%), 65 (32.5%), and 33 (16.5%) cases being classified as stage Ⅰ, stage Ⅱ, and stage Ⅲ, respectively. The clinicopathological characteristics of all patients are summarized in Table 1.

Table 1
Demographic and clinical characteristics of HCC patients.

Factors	**Total Number (n = 200)**	**%**
Gender		
Male	125	62.5
Female	75	37.5
Age (Year)		
Range	22.4 ~ 86.7	
Mean	63.3	
Medium	65.6	
Pre-treatment AFP		
<400ng/ml	62	31.0
≥ 400ng/ml	138	69.0
Tumor size		
<5cm	82	41.0
≥ 5cm	118	59.0
Child-Pugh liver function classification		
A	129	64.5
B	71	35.5
HBsAg		
Positive	143	71.5
Negative	57	28.5
T (T Stage)		
	89	44.5
	48	24.0
	36	18.0
	27	13.5
N (Lymph node)		
N0	189	94.5
N1	11	5.5

Factors	Total Number (n = 200)	%
AJCC cancer stage		
	102	51.0
	65	32.5
	33	16.5
Histological grade		
Well	37	18.5
Moderate	64	32.0
Poor	99	49.5
Liver resection method		
Anatomical liver resection	118	59.0
Non-anatomical liver resection	82	41.0

Expression of SAMM50 in HCC and adjacent normal tissues

IHC staining was performed to evaluate SAMM50 expression in HCC and adjacent normal tissues. As shown in Fig. 1, all patients were divided into low-expression (IRS: 0 ~ 6, n = 100) and high-expression (IRS: 8 ~ 12, n = 100) groups based on the expression of SAMM50. In HCC tissues, SAMM50 was highly expressed in the cytoplasm of liver cancer cells. Microscopic examination showed that HCC cells with negative or weak SAMM50 expression were arranged in a disordered manner, with fewer glandular structures and loss of polarity. These results suggested that high expression of SAMM50 was associated with poor cell differentiation(Fig. 4).

Correlation of SAMM50 expression with clinicopathological factors

To assess the clinical significance of SAMM50 in HCC, the correlation between SAMM50 expression and clinicopathological factors was analyzed (Table 2). qRT-PCR showed that the relative mRNA expression of SAMM50 was significantly higher in HCC tissues than in paired adjacent normal tissues ($P < 0.01$) (Fig. 5A). The data indicate that, compared with normal liver tissue, SAMM50 expression in liver cancer tissue is significantly higher (Fig. 5B). More specifically, its high expression is closely associated with more severe clinical and pathological features, including higher levels of serum alpha-fetoprotein (AFP), larger tumor diameter, later-stage tumor staging (T staging and AJCC staging), lower degree of differentiation, and shorter postoperative survival time for patients (≤ 3 years) (Fig. 5C-H).

However, no significant correlation was observed between SAMM50 expression and sex, age, drinking status, Child–Pugh liver function score, or HbsAg levels (all $P > 0.05$,Table 2). These results validate that SAMM50 has potential prognostic value in HCC.

Table 2
Baseline characteristics of patients with HCC.

Nuclear staining				
Variable	Low	High	(n = 200)	*P*-value
Sex				0.073
Male	68	71	139	
Female	32	29	61	
Age	63.32 ± 12.1	60.5 ± 10.03		0.454
Drinking status				0.545
Yes	73	78	151	
No	27	22	49	
Pre-treatment AFP levels				0.006**
< 400 ng/mL	67(84.8%)	12(15.2%)	79	
≥ 400 ng/mL	33(27.3%)	88(72.7%)	121	
Tumor size				0.004**
< 5 cm	83(70.3%)	35(29.7%)	118	
≥ 5 cm	17(20.8%)	65(79.2%)	82	
Child–Pugh liver function classification				0.077
A	63	66	129	
B	37	34	71	
HBsAg status				0.323
Positive	82	77	159	
Negative	18	23	41	
T stage				0.027*
T1, T2	61 (70.9%)	25 (29.1%)	86	
T3, T4	39 (34.2%)	75 (65.8%)	114	
AJCC stage				0.002*
□, □	63 (70.0%)	27 (30.0%)	90	
* *P* < 0.05, ** *P* < 0.01,*** *P* < 0.001				

Nuclear staining				
□	37 (33.6%)	73 (66.4%)	110	
Histological grade				0.037*
High and moderate	36 (65.5%)	19 (34.5%)	55	
Low	64 (44.1%)	81 (55.9%)	145	
Survival				< 0.001***
< 3 years	44 (35.8%)	79 (64.2%)	123	
≥ 3 years	56 (72.7%)	21 (27.3%)	77	
* $P < 0.05$, ** $P < 0.01$,*** $P < 0.001$				

Independent risk factors influencing the outcomes of HCC

All 200 patients with HCC who underwent liver resection were followed up for 3 ~ 60months. Univariate Cox analysis showed that OS was negatively associated with tumor size, T stage, AJCC cancer stage, pre-treatment AFP levels, drinking status, histological grade, and high SAMM50 expression in patients with HCC ($P < 0.05$ for all; Table 3). Furthermore, multivariate Cox analysis confirmed that high SAMM50 expression, tumor size ≥ 5 cm, high pre-treatment AFP levels, alcohol use, and poor histological grade were independent risk factors for OS in patients with HCC ($P < 0.05$ for all; Table 3).

Table 3
Correlation between SAMM50 expression and clinicopathological characteristics

Variable	Univariate analysis			Multivariate analysis		
	HR	**95% *CI***	***P*-value**	**HR**	**95% *CI***	***P*-value**
Expression of SAMM50			0.003**			0.021*
Low	1.0			1.0		
High	1.6	1.223 ~ 2.332		1.7	1.331 ~ 2.043	
Tumor size			0.014*			0.002**
< 5 cm	1.0			1.0		
≥ 5 cm	1.9	1.176 ~ 3.078		1.4	0.746 ~ 3.176	
T stage			0.009*			0.227
T1, T2	1.0			1.0		
T3, T4	2.8	1.956 ~ 3.887		2.1	0.552 ~ 8.336	
AJCC stage			0.007**			0.596
□, □	1.0			1.0		
□	3.3	2.156 ~ 4.554		1.8	0.276 ~ 5.113	
Pre-treatment AFP levels			< 0.001***			0.005**
< 400 ng/mL	1.0			1.0		
≥ 400 ng/mL	2.4	1.454 ~ 2.767		2.2	1.017 ~ 2.465	
Drinking status			0.022*		1.316 ~ 2.487	0.005**
Yes	1.0			1.0		
No	1.9	1.212 ~ 2.335		2.1	1.316 ~ 2.487	
Histological grade			<0.001***			<0.001***
High	1.0			1.0		

Variable	Univariate analysis			Multivariate analysis		
	HR	95% *CI*	*P*-value	HR	95% *CI*	*P*-value
Moderate and high	1.6	1.018 ~ 2.584		2.3	1.667 ~ 2.732	

Hazard ratio (HR) was adjusted for sex and age ($^{*}P < 0.05$, $^{**}P < 0.01$, $^{***}P < 0.001$).

To evaluate the effectiveness of the discriminatory ability of SAMM50 between liver cancer tissues and normal tissues, ROC curves were generated to assess the discriminative ability of SAMM50. The AUC value of 0.863 indicated that SAMM50 significantly differentiated liver cancer tissues from normal tissues, suggesting its potential as a diagnostic biomarker for HCC (Fig. 6A). Furthermore, a nomogram integrating SAMM50 expression and tumor status was developed to predict the prognosis of HCC. The nomogram was developed based on multivariate Cox regression analysis, with the aim of providing clinicians with a reliable prediction tool. When the predictive performance of the nomogram was compared with that of SAMM50 and tumor status, the C-index was found to be 0.627 (0.537 ~ 0.718) for estimated probabilities ranging from 0.5 to 1.0. According to the nomogram, patients with HCC with a tumor (100 points) and high SAMM50 expression (69 points) would have a total score of 169 points. Survival probabilities at 1, 3, and 5 years were determined by drawing a vertical line downward from the total point scale at 169 and intersecting it with the corresponding value on the outcome axis (Fig. 6B).

The Kaplan–Meier method was used to investigate the relationship between SAMM50 expression and survival outcomes in patients with HCC. In particular, survival rates were compared between the low-and high-SAMM50-expression groups. The results indicated that higher SAMM50 expression was significantly associated with poorer OS ($P = 0.001$; HR [95% CI], 1.47 [1.18 ~ 2.64]) (Fig. 6C), PFS ($P = 0.018$; HR (95% CI), 1.21 [1.01 ~ 1.85]) (Fig. 6D), and DFS ($P = 0.031$; HR [95% CI], 1.32 [1.19 ~ 2.49]) (Fig. 6E). Furthermore, a nomogram was developed to compare the OS of the two groups. The results showed a strong agreement between the predicted and observed survival outcomes in all patients. The nomogram included factors such as tumor size, tumor status, T stage, AJCC stage, histological grade, and SAMM50 expression. The goodness-of-fit of the nomogram was evaluated using the non-significant Hosmer–Lemeshow test (Fig. 6F). Altogether, the findings highlighted the effectiveness of using SAMM50-based models to predict both short - term and long - term survival outcomes in patients with HCC.

The forest plot demonstrates the prognosis of different HCC subtypes(Figure 6G). The results suggest that SAMM50 can be used as a biomarker for predicting survival outcomes in early-stage patients with HCC.

Knockdown of SAMM50 inhibited HCC cell proliferation, migration and facilitated apoptosis

At the cellular level, qRT-PCR and western blot results confirmed that SAMM50 expression was markedly elevated in the LM3, Huh7, and HepG2 cell lines compared to non-malignant LO2 hepatocytes, while it remained unchanged in the HCC-97L and HCC-97H cells (Figs. 7A-B). Together, these data support the notion that SAMM50 is upregulated in HCC and is significantly associated with HCC progression.

Given the strong correlation between SAMM50 expression and HCC progression, particularly its involvement in proliferation-related processes (Fig. 2F, GOand KEGG analyses), we sought to examine the functional role of SAMM50 in HCC cells. To this end, we knocked down (KD) SAMM50 expression in Huh7 and HepG2 cells using two independent siRNAs (siSAMM50-1 and siSAMM50-2). qRT-PCR and western blot results confirmed the efficient depletion of SAMM50 at both the mRNA and protein levels in both cell lines (Figs. 7C–D). The CCK-8 experiment indicated that knockdown of SAMM50 significantly inhibited the proliferation of Huh7 and HepG2 cells (Fig. 7E). Furthermore, colony formation assays demonstrated that SAMM50 depletion significantly suppressed the clonogenic capacity of Huh7 and HepG2 cells (Figs. 7F-G). The scratch test showed that the knockdown of SAMM50 markedly suppressed the migration ability of Huh7 and HepG2 cells (Figs. 7H-I). Finally, flow cytometry results demonstrated that the knockdown of SAMM50 dramatically increased the apoptotic ratio of Huh7 and HepG2 cells (Figs. 7J-K). These data indicated that SAMM50 is a pro-oncogene, and inhibiting its expression could inhibit the malignant biological processes of HCC cells.

SAMM50 knockdown suppressed HCC growth in vivo

To extend these findings in vivo, we constructed stable SAMM50-KD Huh7 cells using a lentiviral shRNA system (Fig. 8A) and subcutaneously implanted them into nude mice. Consistent with the in vitro results, SAMM50 KD substantially inhibited tumor growth (Figs. 8B-E). Collectively, these data indicate that SAMM50 is critical for HCC cell proliferation, as its depletion significantly hampers proliferation both in *vitro* and in *vivo*.

Discussion

HCC is a prevalent malignant tumor that poses a significant global health risk owing to its aggressive nature, high mortality rates, and poor prognosis[22, 23]. The pathogenesis of HCC is complex, involving factors such as hepatitis virus infection, epigenetic alterations, mitochondrial dysfunction, and signaling pathway dysregulation[24–26]. Despite ongoing research, the precise mechanisms underlying the development and recurrence of HCC remain elusive.

Owing to the absence of prognostic biomarkers, postoperative recurrence is often detected late in some patients, and the opportunity for prompt and appropriate treatment is missed[27–29]. Therefore, identifying effective biomarkers for early diagnosis and postoperative HCC recurrence prognosis is necessary to improve patient management and outcomes. In addition, identifying novel therapeutic targets is crucial to overcoming the limitations of existing treatment strategies. These targets may be used to develop precise, individualized treatment approaches, thereby enhancing therapeutic efficacy.

In this study, we analyzed the relationship between SAMM50 expression and several clinicopathological factors in HCC patients. Table 2 indicates that high SAMM50 expression is closely associated with more aggressive tumor behaviors (such as large tumor size, advanced stage, poor differentiation, high AFP, and short-term mortality), and this association is not affected by age, sex, or liver function status, suggesting its potential as a prognostic marker. These results suggest that high SAMM50 expression contributes to HCC progression.

Studies investigating the clinical significance of SAMM50 in HCC are limited. To the best of our knowledge, this study is the first to demonstrate that SAMM50 is upregulated in HCC tissues and serves as a promising diagnostic and prognostic biomarker for HCC. Studies have shown that SAMM50 loss triggers phosphatidylserine externalization, Bax recruitment to mitochondria, and subsequent mtDNA release, resulting in changes to the tumor immune microenvironment[30]. These alterations may contribute to nonalcoholic fatty liver disease and liver injury, both well-known risk factors for HCC[31, 32]. In this study, high SAMM50 expression in HCC tissues was associated with aggressive tumor behavior; however, the precise mechanism by which SAMM50 contributes to HCC development warrants further investigation.

IHC analysis and qRT-PCR showed that SAMM50 expression was significantly higher in HCC tissues than in adjacent normal tissues (Figs. 1 and 2A). Taken together, SAMM50 acts as an oncogene in HCC and demonstrates potential as a diagnostic biomarker for distinguishing HCC from normal liver tissue. Furthermore, high SAMM50 expression was correlated with poor survival outcomes, indicating its potential as a therapeutic target for HCC. High SAMM50 expression was significantly associated with elevated pre-treatment AFP levels, larger tumor size, advanced T stage and AJCC stage, poor histological grade, and reduced OS (all $P < 0.05$;Figures 5C-H). Subsequently, a nomogram integrating SAMM50 expression and several clinicopathological factors was developed to predict HCC prognosis in clinical settings (Fig. 6B).

Clinical studies have shown that metastasis and recurrence critically impact postoperative survival of HCC patients[33, 34]. Despite safe radical resection, the postoperative recurrence rate remains alarmingly high, ranging from 50% to 80%[35, 36]. Existing postoperative monitoring practices primarily rely on AFP level assessment and imaging. However, due to limitations associated with these practices, postoperative recurrence detection and accurate prognosis assessment are often delayed, and the optimal treatment window is missed[37, 38]. Therefore, identifying proteins and molecular mechanisms associated with HCC pathogenesis is necessary. In this study, univariate analysis showed that tumor size, T stage, AJCC stage, pre-treatment AFP levels, alcohol use, histological grade, and high SAMM50 expression significantly affected OS in HCC patients (Table 3). Furthermore, multivariate Cox regression validated that high pre-treatment AFP levels, tumor size ≥ 5 cm, alcohol use, poor histological grade, and high SAMM50 expression were independent prognostic risk factors for postoperative HCC patients. These results indicate that high SAMM50 expression is associated with aggressive tumor behavior and unfavorable prognosis in HCC patients.

This study integrates HCC clinicopathological factors with SAMM50 expression to assess prognostic value. The rapid proliferation of cancer cells necessitates high energy generation, facilitated through anaerobic glucose breakdown and mitochondrial oxidative phosphorylation. Furthermore, increased mitochondrial production of reactive oxygen species (ROS) sustains cancer cell survival and substantially promotes malignancy progression in solid tumors[39]. Although increased ROS levels may be an essential mechanism through which SAMM50 contributes to HCC development, the specific mechanism warrants further investigation.

Kaplan-Meier analysis with the log-rank test showed that OS, PFS, and DFS rates were significantly lower in patients with high SAMM50 expression ($P < 0.05$ or $P < 0.01$) (Figs. 3C-E). These results suggest that SAMM50 is a reliable biomarker for assessing postoperative prognosis in HCC patients. In addition, the nomogram integrating SAMM50 expression and several clinicopathological factors showed high accuracy and robustness in predicting the prognosis of HCC (Fig. 6B). Cox regression analysis was used to generate a forest plot using R software to further elucidate clinicopathological features associated with SAMM50 expression for HCC prognosis (Fig. 4). These tools provide valuable insights into the relationship between SAMM50 expression and HCC prognosis.

Nevertheless, the function of SAMM50 had not been studied in HCC prior to this work. Therefore, we first investigated the function of SAMM50 using loss-of-function assays in vitro. The experimental data indicated that SAMM50 knockdown inhibited proliferation, migration, and invasion and promoted apoptosis in HepG2 and Huh7 cells. In addition, we validated these findings in an animal model. The observed trends were consistent with the cellular-level findings. These results indicate that SAMM50 participates in regulating malignant biological processes in HCC cells.

In conclusion, this study revealed that SAMM50 expression is remarkably high in HCC tissues and is associated with poor survival outcomes. Additionally, SAMM50 was identified as an independent predictor of postoperative survival in HCC patients. Nomograms and forest plots validated the reliability and clinical relevance of these findings, suggesting that SAMM50 serves as a valuable diagnostic and prognostic biomarker and a promising therapeutic target for HCC.

Despite these important findings, this study has several limitations that should be acknowledged. First, this study employed a single-center, retrospective design with a modest sample size, which may have introduced bias. Second, the surgical data of HCC patients were collected from multiple surgeons. Consequently, variations in surgical approaches and techniques might have influenced postoperative outcomes and confounded the results.

Conclusion

In summary, this study demonstrates that SAMM50 is significantly upregulated in HCC and its high expression predicts poor clinical outcomes. SAMM50 was identified as an independent prognostic factor for postoperative HCC patients. Functional experiments confirmed that SAMM50 knockdown

suppresses HCC malignant behaviors in vitro and in vivo. These findings suggest that SAMM50 serves as a valuable diagnostic and prognostic biomarker and a potential therapeutic target for hepatocellular carcinoma.

Declarations

Ethics approval and consent to participate: All aspects of this study were approved by the Research Ethics Committee of the Third Affiliated Hospital of Wenzhou Medical University.

Consent for publication: Informed consent was obtained from all subjects involved in the study.

Data Availability Statement: The datasets generated in the current study are available from the corresponding authors on reasonable request.

Conflict of interest disclosure: The authors have no relevant financial or non-financial interests to disclose.

Funding: This work was supported by Innovation Special Fund of Ruian Science and Technology Bureau (Grant No. MS2024001).Medical and Health Science Program of Zhejiang Province (Grant No. 2025HY1115).Wenzhou Municipal Science and Technology Bureau Applied Basic Research Project (Grant No. GK2025117).

Authorship contribution: All authors contributed to the study conception and design. Material preparation, data collection and analysis were performed by Huawei Zhai, Banglian Cai, Zihao Zheng, Fujing Cai、Zhen miaoWan、Yuchen Pan、Guangzheng Sunand Haifeng Zhang. The first draft of the manuscript was written by Jinhai Li, and all authors commented on previous versions of the manuscript. All authors read and approved the final manuscript.

Acknowledgement: The authors thank all patients who participated in this study. We appreciate the support from the Department of Hepatobiliary Pancreatic Surgery and the Experimental Research Center at the Third Affiliated Hospital of Wenzhou Medical University. No external funding was received for this research.

References

1. Rui T, Zhang X, Guo J, Xiang A, Tang N, Liu J, et al. **Serum-Exosome-Derived miRNAs Serve as Promising Biomarkers for HCC Diagnosis**. *Cancers (Basel),* 2022; 15(1):775-792.
2. Qian F, Wang J, Wang Y, Gao Q, Yan W, Lin Y, et al. **MiR-378a-3p as a putative biomarker for hepatocellular carcinoma diagnosis and prognosis: Computational screening with experimental validation**. *Clin Transl Med* , 2021; 11(2):e307-e321.
3. Sogbe M, Bilbao I, Marchese FP, Zazpe J, De Vito A, Pozuelo M, et al. **Prognostic value of ultra-low-pass whole-genome sequencing of circulating tumor DNA in hepatocellular carcinoma under**

systemic treatment. *Clin Mol Hepatol ,* 2024; 30(2):177-190.

4. Guo W, Zhang J, Zhang D, Cao S, Li G, Zhang S, et al. **Polymorphisms and expression pattern of circular RNA circ-ITCH contributes to the carcinogenesis of hepatocellular carcinoma**. *Oncotarget,* 2017; 8(29):48169-48177.
5. Wang X, He Y, Mackowiak B, Gao B. **MicroRNAs as regulators, biomarkers and therapeutic targets in liver diseases**. *Gut,* 2021; 70(4):784-795.
6. Leettola CN, Knight MJ, Cascio D, Hoffman S, Bowie JU. **Characterization of the SAM domain of the PKD-related protein ANKS6 and its interaction with ANKS3**. *BMC Struct Biol,* 2014; 14(17):10233-10249.
7. Vincenzi M, Mercurio FA, Leone M. **Sam Domains in Multiple Diseases**. *Curr Med Chem,* 2020; 27(3):450-476.
8. Chen L, Dong J, Liao S, Wang S, Wu Z, Zuo M, et al. **Loss of Sam50 in hepatocytes induces cardiolipin-dependent mitochondrial membrane remodeling to trigger mtDNA release and liver injury**. *Hepatology,* 2022; 76(5):1389-1408.
9. Chen Z, Tian R, She Z, Cai J, Li H. **Role of oxidative stress in the pathogenesis of nonalcoholic fatty liver disease**. *Free Radic Biol Med,* 2020; 152(1):116-141.
10. Chiusolo V, Jacquemin G, Yonca Bassoy E, Vinet L, Liguori L, Walch M, et al. **Granzyme B enters the mitochondria in a Sam50-, Tim22- and mtHsp70-dependent manner to induce apoptosis**. *Cell Death Differ,* 2017; 24(4):747-758.
11. Bakey Z, Bihoreau MT, Piedagnel R, Delestré L, Arnould C, de Villiers A, et al. **The SAM domain of ANKS6 has different interacting partners and mutations can induce different cystic phenotypes**. *Kidney Int,* 2015; 88(2):299-310.
12. Rao Z, Li F, Guan Z, Zhou H. **Letter to the editor: Loss of Sam50 in hepatocytes induces cardiolipin-dependent mitochondrial membrane remodeling to trigger mtDNA release and liver injury**. *Hepatology,* 2022; 76(5):E94-E95.
13. Kitamoto T, Kitamoto A, Yoneda M, Hyogo H, Ochi H, Nakamura T, et al. **Genome-wide scan revealed that polymorphisms in the PNPLA3, SAMM50, and PARVB genes are associated with development and progression of nonalcoholic fatty liver disease in Japan**. *Hum Genet,* 2013; 132(7):783-792.
14. Chan NC, Lithgow T. **The peripheral membrane subunits of the SAM complex function codependently in mitochondrial outer membrane biogenesis**. *Mol Biol Cell,* 2008; 19(1):126-136.
15. Wang Q, Guan Z, Qi L, Zhuang J, Wang C, Hong S, et al. **Structural insight into the SAM-mediated assembly of the mitochondrial TOM core complex**. *Science,* 2021; 373(6561):1377-1381.
16. Kumar VB, Lee CH, Su TC, Lin CC, Mohammedsaleh ZM, Yeh CM, et al. **Prognostic and Clinical Implications of UNC13C expression in Hepatocellular Carcinoma Patients**. *Int J Med Sci,* 2023; 20(9):1235-1239.
17. Kołodziej-Rzepa M, Biesaga B, Słonina D, Mucha-Małecka A. **Nanog expression in patients with squamous cell carcinoma of oropharynx in relation to immunohistochemical score**. *Pol J Pathol,* 2022; 73(1):60-71.

18. Dong Z, Li J, Dai W, Yu D, Zhao Y, Liu S, et al. **RRP15 deficiency induces ribosome stress to inhibit colorectal cancer proliferation and metastasis via LZTS2-mediated β-catenin suppression**. *Cell Death Dis,* 2023; 14(2):89-103.
19. Lin H, Han Q, Wang J, Zhong Z, Luo H, Hao Y, et al. **Methylation-Mediated Silencing of RBP7 Promotes Breast Cancer Progression through PPAR and PI3K/AKT Pathway**. *J Oncol,* 2022; 20(8):9039110-9039121.
20. Li J, Qian L, Ge M, Zhao J, Yang Y. **hsa_circ_0000518 stimulates the malignant progression of hepatocellular carcinoma via regulating ITGA5 to activate the Warburg effect**. *Cell Signal,* 2024; 120(8):111243-111258.
21. Tang J, Zhang K, Dong J, Yan C, Hu C, Ji H, et al. **Sam50-Mic19-Mic60 axis determines mitochondrial cristae architecture by mediating mitochondrial outer and inner membrane contact**. *Cell Death Differ,* 2020; 27(1):146-160.
22. Koshy A. **Evolving Global Etiology of Hepatocellular Carcinoma (HCC): Insights and Trends for 2024**. *J Clin Exp Hepatol,* 2025; 15(1):102406-102420.
23. Kocjan J, Rydel M, Adamek M. **Hepatocellular Carcinoma (HCC) Metastasis to the Diaphragm Muscle: A Systematic Review and Meta-Analysis of Case Reports**. *Cancers (Basel),* 2024; 16(17):111350-111368.
24. Cohen-Naftaly M, Simon R, Lubezky N, Braun M, Khalaileh A, Safadi R, et al. **[HCC TRANSPLANT CANDIDATES' SURVIVAL ON THE WAITING LIST - CAN ORGAN UTILIZATION BE IMPROVED?]**. *Harefuah,* 2023; 162(5):295-298.
25. Lu F, Ott C, Bista P, Lu X. **Three-Dimensional Structure of Novel Liver Cancer Biomarker Liver Cancer-Specific Serine Protease Inhibitor Kazal (LC-SPIK) and Its Performance in Clinical Diagnosis of Hepatocellular Carcinoma (HCC)**. *Diagnostics (Basel),* 2024; 14(7):679-692.
26. Kwei-Nsoro R, Attar B, Ojemolon PE, Annor EN, Go B. **A Curious Case of Vanishing Hepatocellular Carcinoma (HCC)**. *Cureus,* 2023; 15(10):e46576-e46589.
27. Alawyia B, Constantinou C. **Hepatocellular Carcinoma: a Narrative Review on Current Knowledge and Future Prospects**. *Curr Treat Options Oncol,* 2023; 24(7):711-724.
28. Temraz S, Nassar F, Kreidieh F, Mukherji D, Shamseddine A, Nasr R. **Hepatocellular Carcinoma Immunotherapy and the Potential Influence of Gut Microbiome**. *Int J Mol Sci,* 2021; 22(15):13206-13225.
29. Ganne-Carrié N, Nahon P. **Differences between hepatocellular carcinoma caused by alcohol and other aetiologies**. *J Hepatol* 2025; 82(5):909-917.
30. Nischalke HD, Schmalz F, Buch S, Fischer J, Möller C, Matz-Soja M, et al. **Genetic Variation of SAMM50 Is Not an Independent Risk Factor for Alcoholic Hepatocellular Carcinoma in Caucasian Patients**. *Int J Mol Sci,* 2022; 23(23):20135-20147.
31. Li X, Chen S, Shi Y, Wang Y, Wang X, Lin Q, et al. **Transcription factor MEF2D regulates aberrant expression of ACSL3 and enhances sorafenib resistance by inhibiting ferroptosis in HCC**. *Front Pharmacol,* 2024; 15(8):1464852-1464875.

32. Brozzetti S, Tancredi M, Bini S, De Lucia C, Antimi J, D'Alterio C, et al. **HCC in the Era of Direct-Acting Antiviral Agents (DAAs): Surgical and Other Curative or Palliative Strategies in the Elderly**. *Cancers (Basel),* 2021; 13(12):33658-33672.
33. Lee PC, Wu CJ, Hung YW, Lee CJ, Mon HC, Chi CT, et al. **Distinct gut microbiota but common metabolomic signatures between viral and MASLD HCC contribute to outcomes of combination immunotherapy**. *Hepatology,* 2025,13(10):13879-13892.
34. Moudi B, Mohades MR, Mahmoudzadeh-Sagheb H, Heidari Z. **Immunohistochemical expression of CB1 receptors in the liver of patients with HBV related-HCC**. *Arab J Gastroenterol,* 2023; 24(1):34-39.
35. Wang Y, Zhao Z, Guo T, Wu T, Zhang M, Luo D, et al. **SOCS5-RBMX stimulates SREBP1-mediated lipogenesis to promote metastasis in steatotic HCC with HBV-related cirrhosis**. *NPJ Precis Oncol,* 2024; 8(1):58-78.
36. Beudeker BJB, Guha R, Stoyanova K, JNM IJ, de Man RA, Sprengers D, et al. **Cryptogenic non-cirrhotic HCC: Clinical, prognostic and immunologic aspects of an emerging HCC etiology**. *Sci Rep,* 2024; 14(1):4302-4322.
37. Tang B, Wang Y, Zhu J, Song J, Fang S, Weng Q, et al. **TACE responser NDRG1 acts as a guardian against ferroptosis to drive tumorgenesis and metastasis in HCC**. *Biol Proced Online,* 2023; 25(1):13-27.
38. Yu B, Ma W. **Biomarker discovery in hepatocellular carcinoma (HCC) for personalized treatment and enhanced prognosis**. *Cytokine Growth Factor Rev,* 2024; 79:29-38.
39. Vadevoo SMP, Kang Y, Gunassekaran GR, Lee SM, Park MS, Jo DG, et al. **IL4 receptor targeting enables nab-paclitaxel to enhance reprogramming of M2-type macrophages into M1-like phenotype via ROS-HMGB1-TLR4 axis and inhibition of tumor growth and metastasis**. *Theranostics,* 2024; 14(6):2605-2621.

Figures

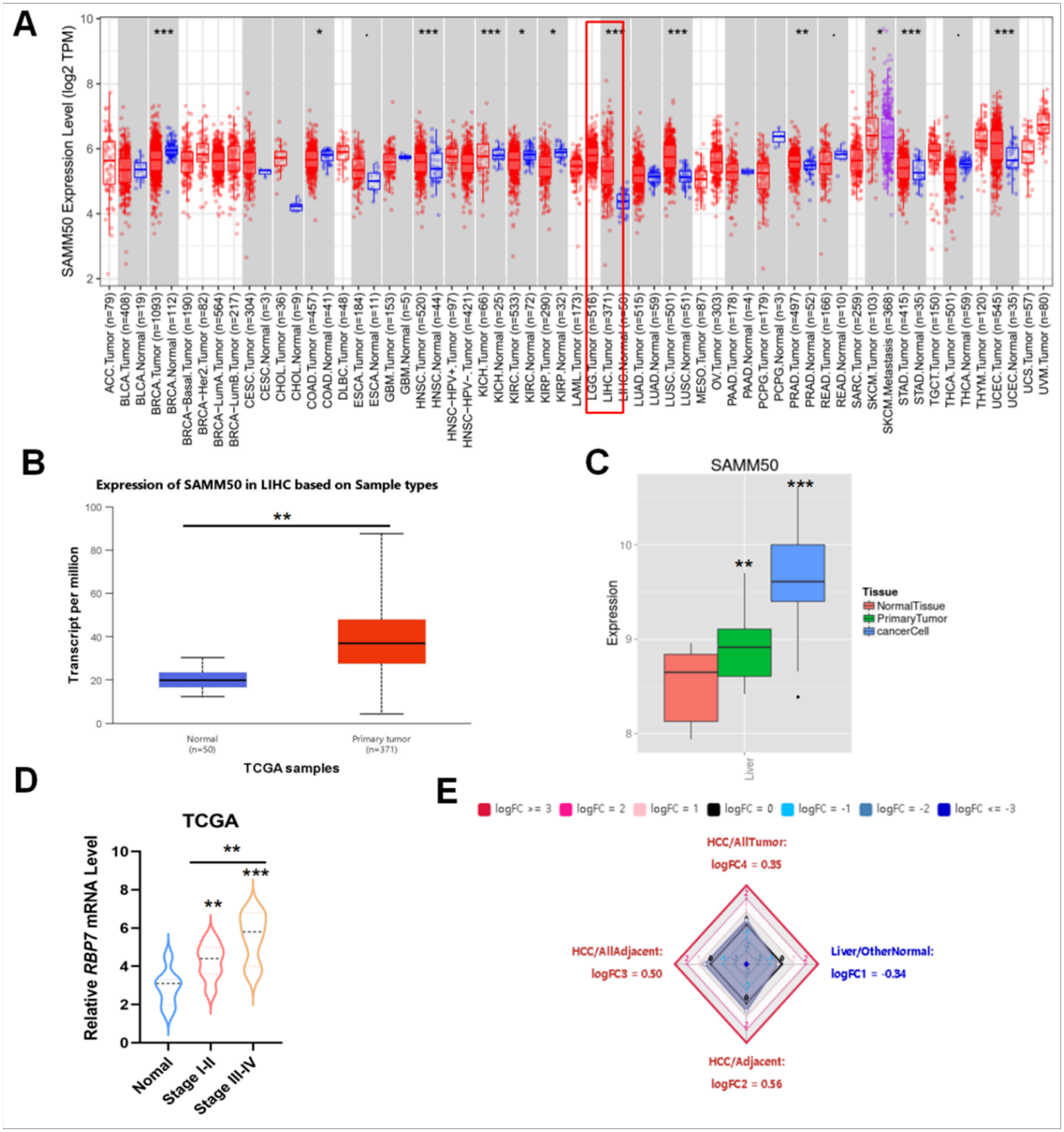

Figure 1

SAMM50 is frequently elevated in HCC tissues. (**A**) Expression of SAMM50 mRNA across different types of cancer based on TCGA cohorts. (**B**) Expression of SAMM50 in HCC was analyzed using CPTAC cohorts.(**C**) The mRNA expression level of SAMM50 was significantly higher in HCC cells and Primary liver tissues than that in normal tissues in the MERAV.(**D**)Expression of SAMM50 mRNA in different

stages of HCC patients using TCGA cohorts.(**E**)Radar map of SAMM50 overall expression among different types of tissues.

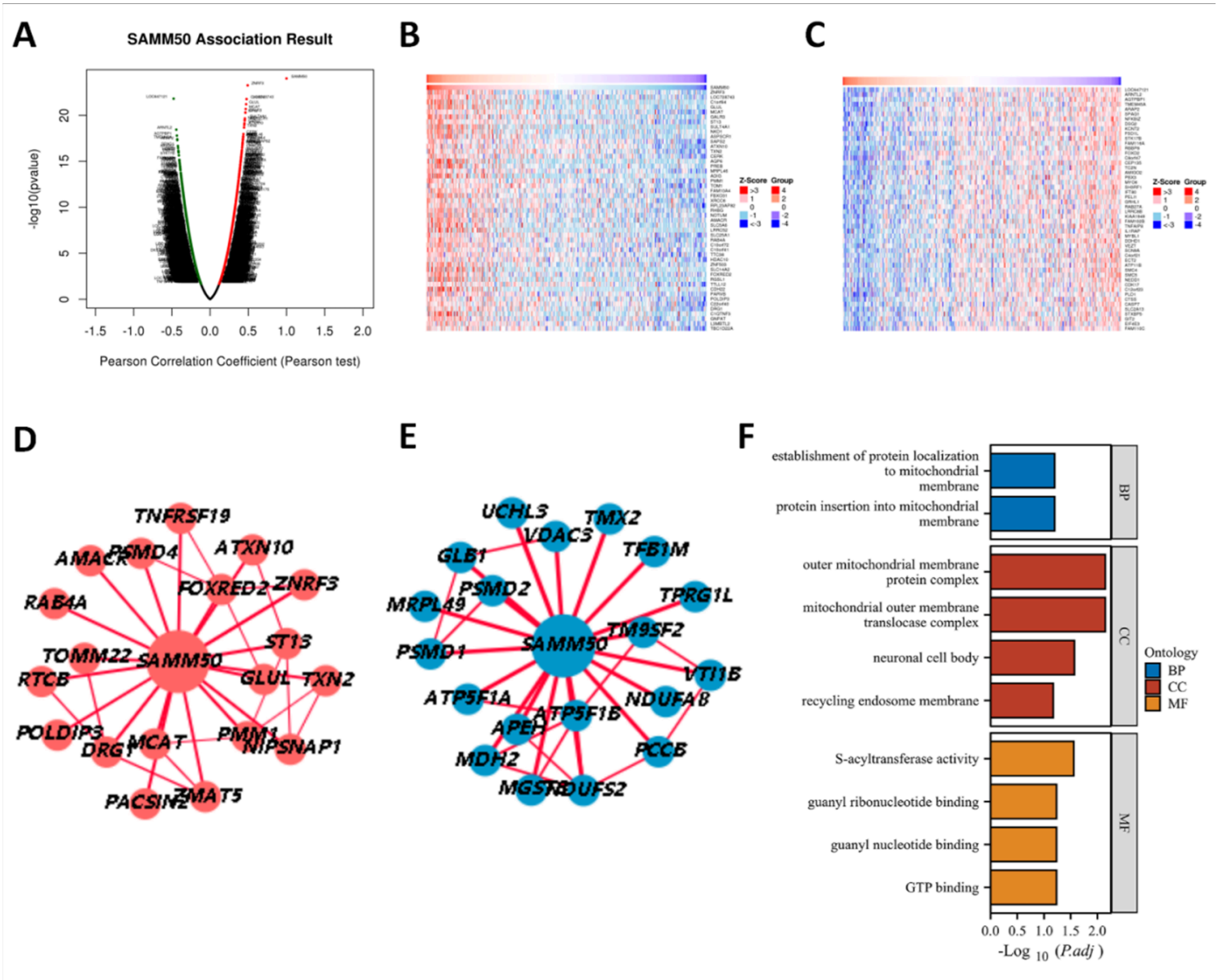

Figure 2

Co-expressed genes of SAMM50 and its GO and KEGG analyses in HCC. (**A**) Genes correlated with SAMM50 showing in volcano plot; red (positive), green (negative). (**B-C**) Heat maps showing the top 50 genes positively and negatively correlated with SAMM50 in HCC.(**D**) The co-expression networks of SAMM50 in HCC tissues. (**E**) The co-expression networks of SAMM50 in adjacent liver tissues. (**F**) GO and KEGG enrichment analyses of genes co-expressed in HCC tissues and adjacent liver tissues.

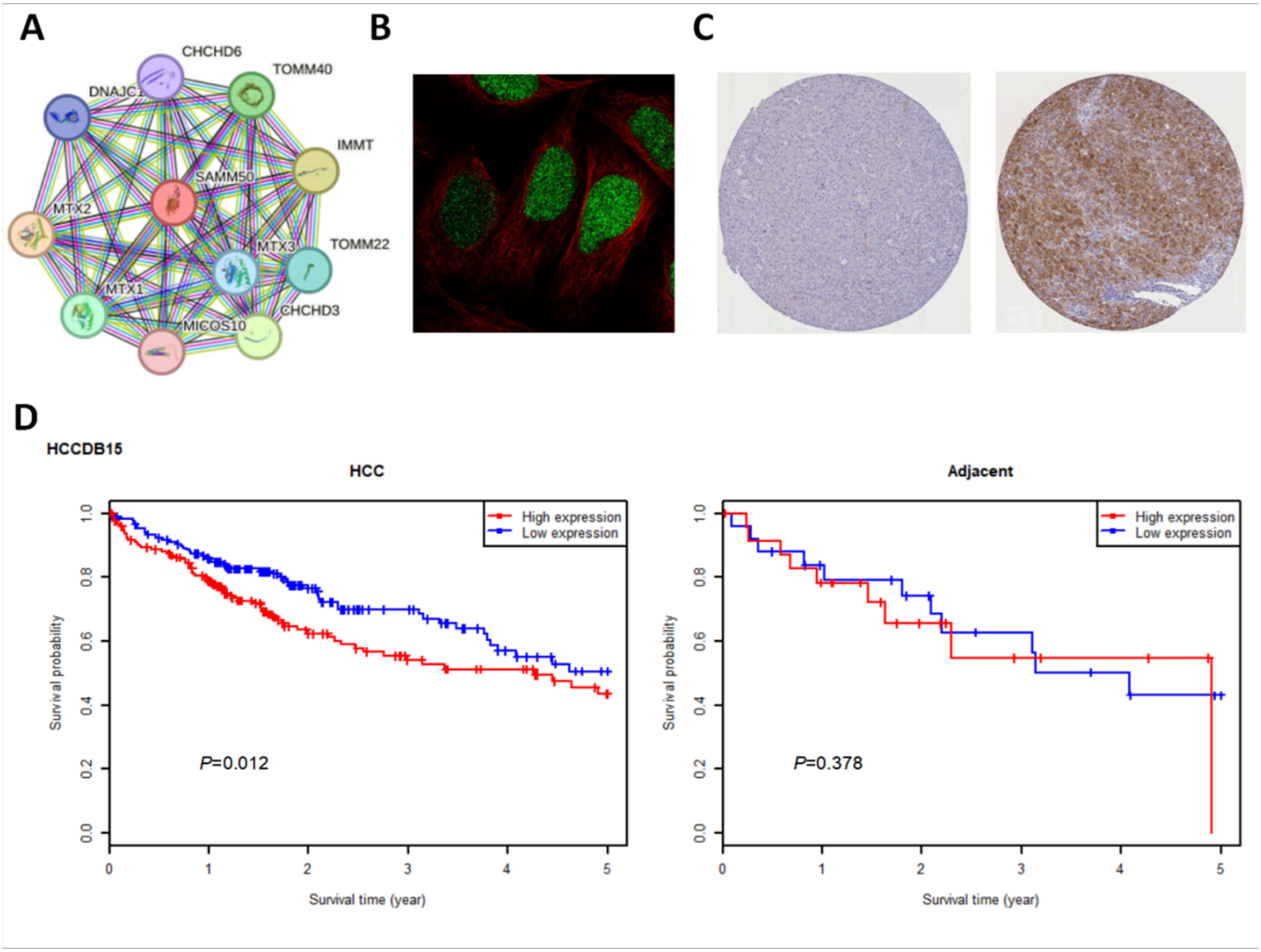

Figure 3

"PPI network" of SAMM50 in HCC patients and the correlation between the expression of SAMM50 mRNA with overall survival in HCC.(**A**) PPI of SAMM50 and other interacting proteins. (**B**) Subcellular localization of SAMM50 in human cells from the HPA database. (**C**) Immunohistochemistry staining showing the differential expression of SAMM50 in liver cancer tissues and adjacent non-tumor tissues from the HPA database. Note: The red fluorescence represents the cell skeleton, the green fluorescence represents SAMM50, and the blue fluorescence represents the cell nucleus.**D**In the HCC tissues, the survival probability of the group with high expression of SAMM50 decreased at a significantly faster rate compared to that of the group with low expression. However, in the adjacent tissues, there was no significant difference in the survival curves between the two groups of patients.

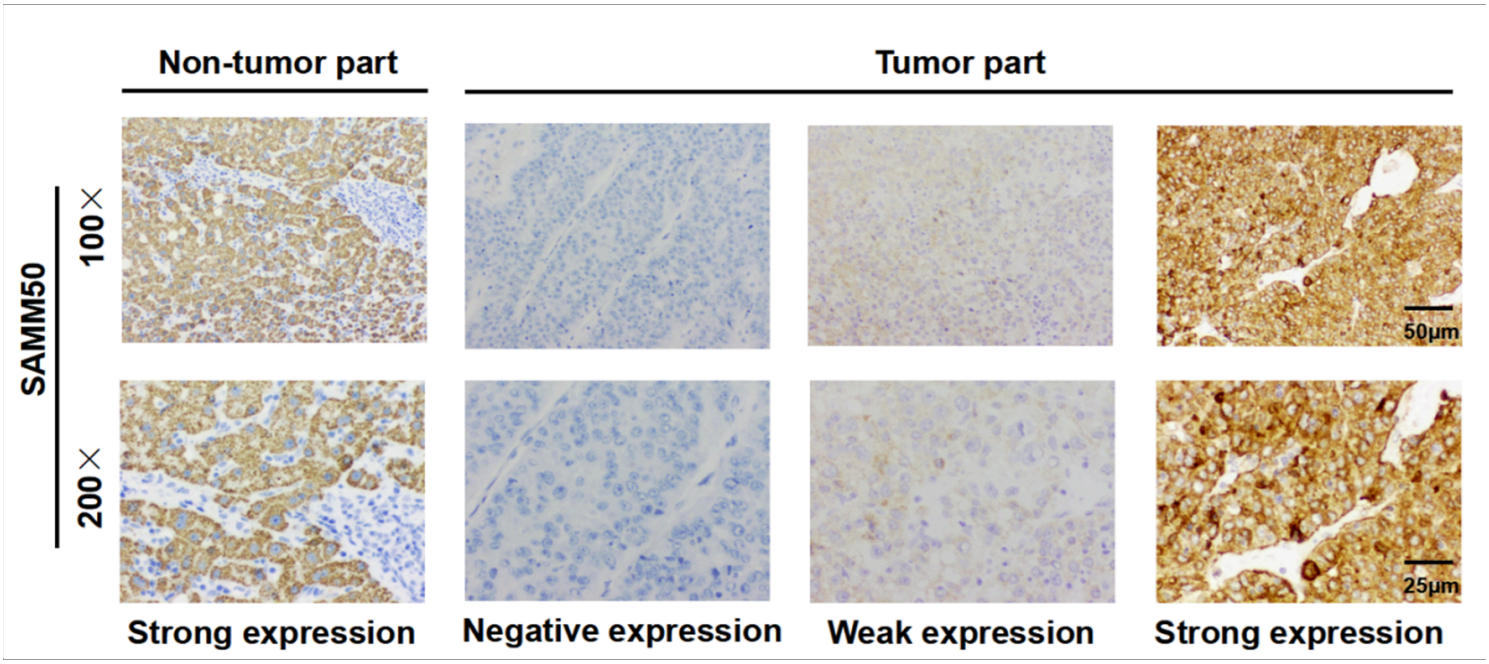

Figure 4

The protein expression of SAMM50 in HCC tissues was analyzed via immunohistochemical staining. Magnification: top panel, 100×; higher panel, 200×.Scale bars =25 and 50 μm.

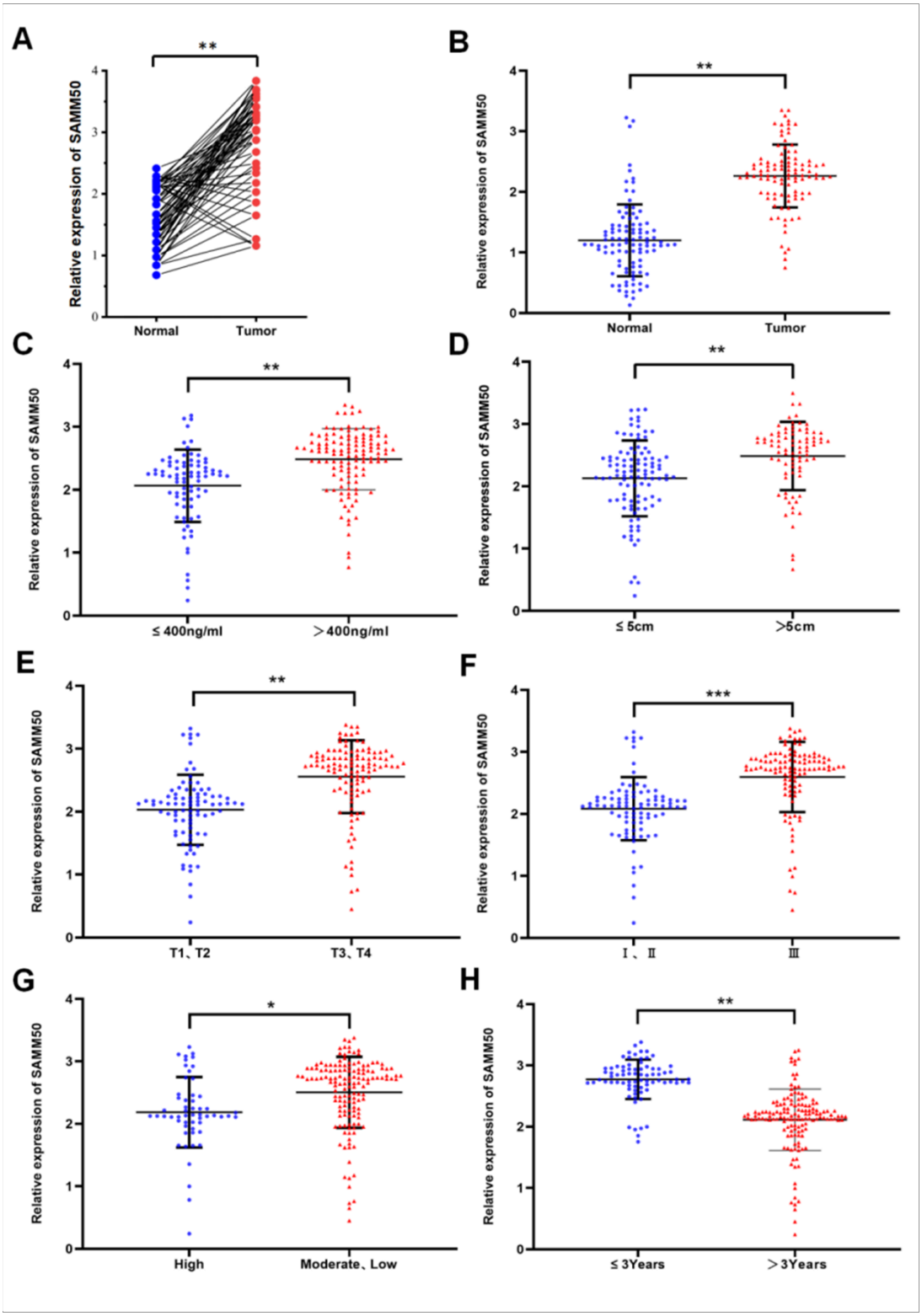

Figure 5

Expression analysis of SAMM50 mRNA in clinical samples was calculated. (**A**) SAMM50 expression was significantly higher in HCC tissues than in matched tissues according to the qRT-PCR experiment. (**B**) The overall expression level of SAMM50 was significantly higher in HCC tissues than in adjacent normal tissues. (**C**) high SAMM50 expression was associated with high pre-treatment AFP levels. (**D**) high SAMM50 expression was associated with large tumor size. (**E**) high SAMM50 expression was

associated with advanced T stage. (**F**) high SAMM50 expression was associated with advanced AJCC stage. (**G**) high SAMM50 expression was associated with a poor histological grade. (**H**) High SAMM50 expression was associated with poor survival ($^{***}P < 0.001$; $^{**}P < 0.01$; $^{*}P < 0.05$).

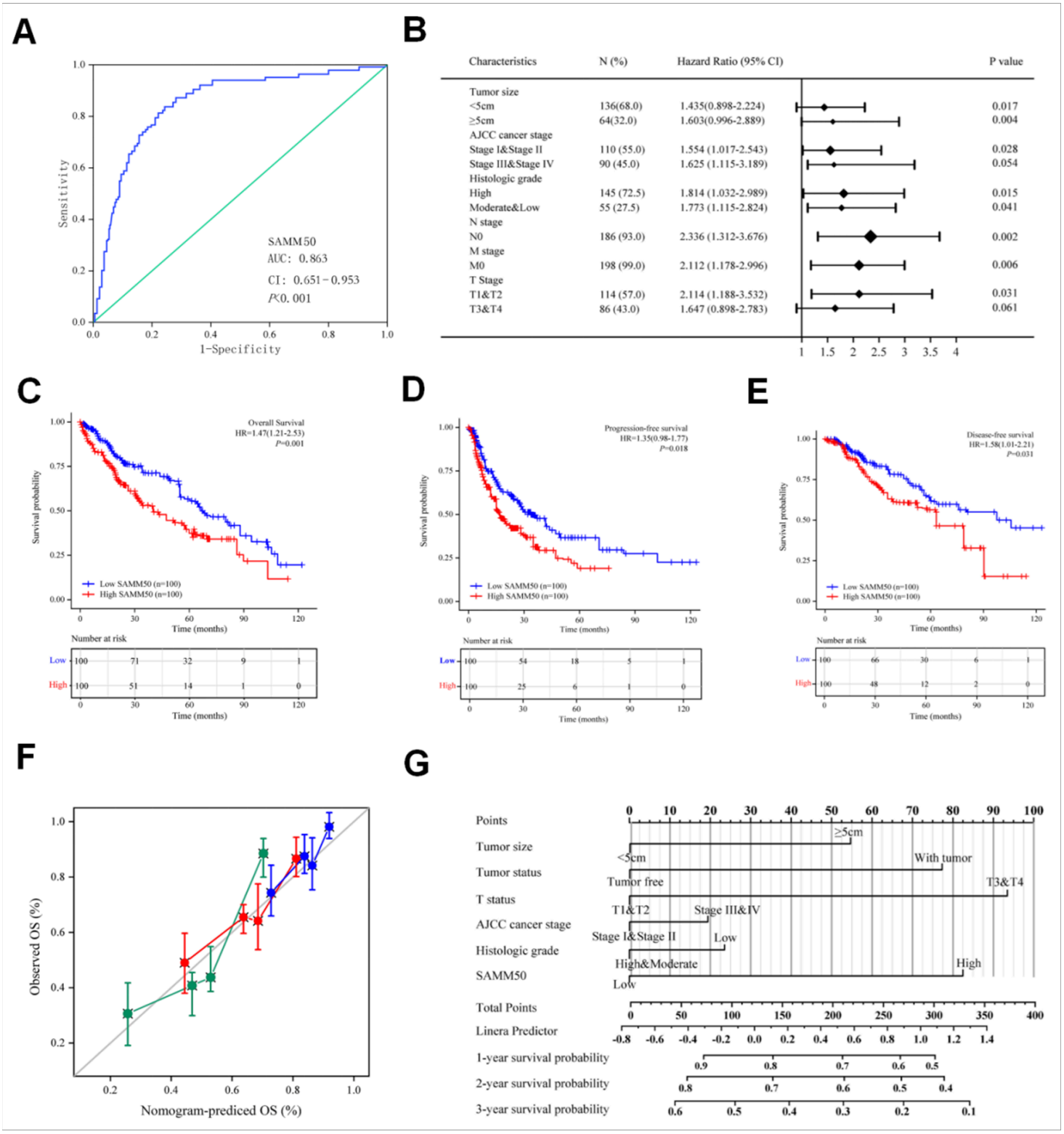

Figure 6

Effective nomogram model for assessing the prognostic relevance of SAMM50 in HCC. (**A**) ROC analysis demonstrated that SAMM50 had a high ability to discriminate between HCC tissues and adjacent normal tissues. The X-axis represents the false-positive rate (FPR), whereas the Y-axis represents the true positive rate (TPR). AUC values are plotted as sensitivity (%) vs specificity (%). (**B**) Nomogram for predicting survival probability at 1, 2, and 3 years in patients with HCC. (C–E) high SAMM50 expression was associated with poor (**C**) overall survival (OS), (**D**) progression-free survival (PFS), and (**E**) disease-free survival (DFS) in patients with HCC. Blue: low expression; Red: high expression (* $P < 0.05$; ** $P < 0.01$). (**F**) Calibration curve with Hosmer–Lemeshow test of the nomogram-predicted OS (%) associated with SAMM50 expression, tumor size, tumor status, T stage, AJCC stage, and histological grade. The X-axis represents the predicted survival rate (0–100%), whereas the Y-axis represents the observed OS rate (0–100%). The gray line represents the ideal line. (**G**) Forest map demonstrating subtypes of clinicopathological features associated with SAMM50 expression for HCC prognosis ($^{*}P < 0.05$; $^{**}P < 0.01$).

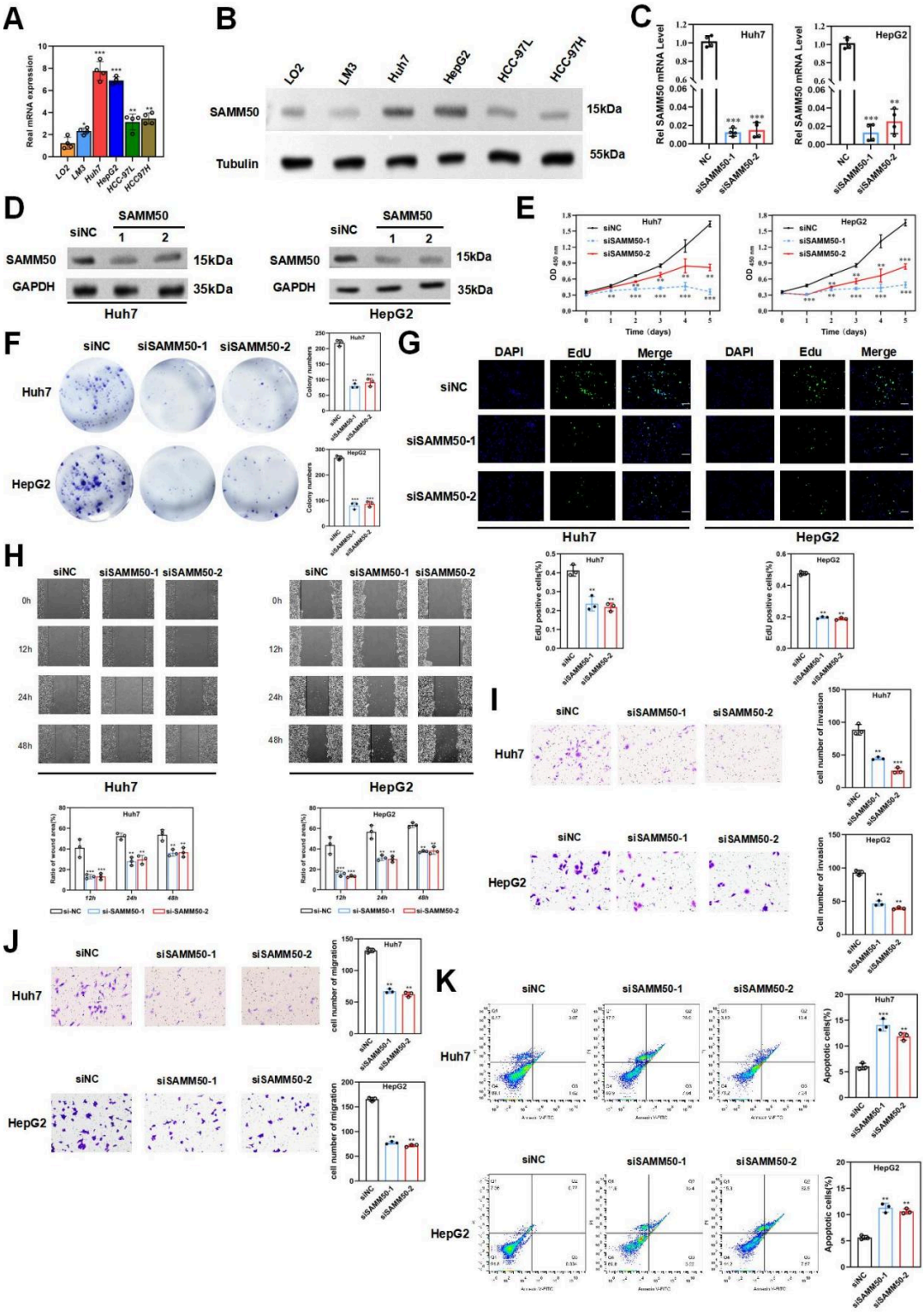

Figure 7

Knockdown of SAMM50 inhibited HCC cell proliferation, migration and promoted apoptosis in vitro. **A-B** qRT-PCR (A) or western blot (B) results showing SAMM50 expression in normal hepatocytes LO2 cells and HCC cells. **C-D** qRT-PCR (**C**) or western blot (**D**) results showing the expression of SAMM50 in Huh7 and HepG2 cells after transfection with indicated siRNA.(**E**) CCK8 assays were applied to examine the proliferation capacity of Huh7 and HepG2 cells after SAMM50 KD. (**F**) Colony formation assays were

applied to assess the cell colony formation ability of Huh7 and HepG2 cells after SAMM50 KD.,and colony numbers were counted by Image J software and relative colony number were calculated.(**G**)EdU determination for cell proliferation. Green, EdU; blue, DAPI; scale bar, 50 μm. Proliferation index was expressed as percentage of EdU positive cells to total nuclei.(**H**)Scratch assays were applied to examine the cell migration ability of Huh7 and HepG2 cells after SAMM50 KD.(**I**)Transwell invasion assay. Scale bar, 100 μm. (**J**)Transwell migration assay. Scale bar, 100 μm. (**K**)Flow cytometric assay was applied to examine the apoptosis of Huh7 and HepG2 cells after SAMM50 knockdown. All experiments, except the xenograft tumor assay, were performed at least three times. Data are shown as mean ± standard deviations. *P* values were determined by Student's *t* test; $^{*}P< 0.05$, $^{**}P< 0.01$ and $^{***}P< 0.001$.

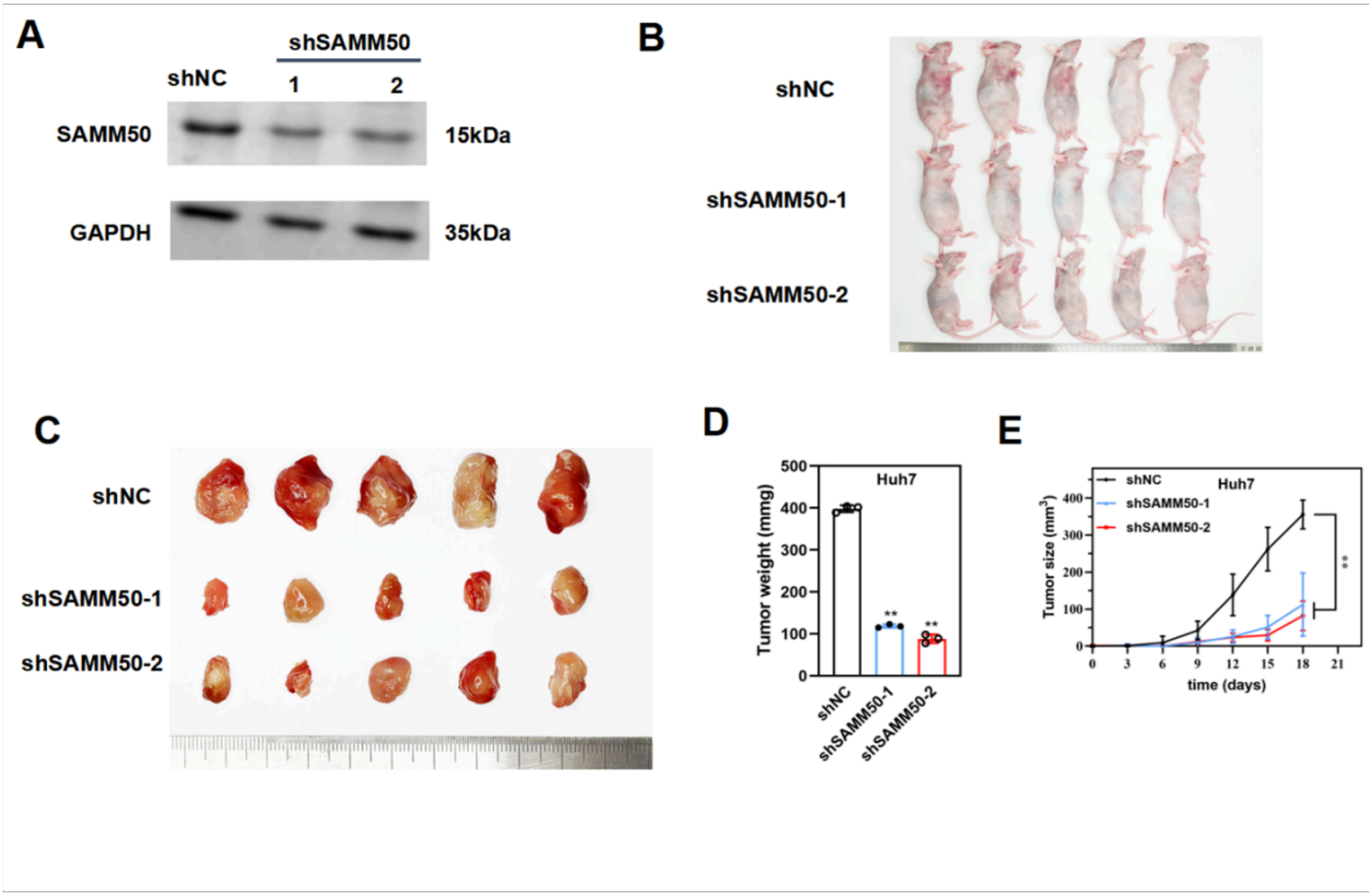

Figure 8

Knockdown of SAMM50 suppressed HCC growth in *vivo*.(**A**)Western blot result showing the expression of SAMM50 in Huh7 and HepG2 cells after transfection with indicated siRNA.(**B-C**) Tumor pictures of SAMM50 knockdown subcutaneous tumor model mice.**(D)** The tumor tissues of the shRNA (transfected with shRNA-NC) and shSAMM50 (transfected with SAMM shRNA1,2) groups were weighed. **(E)** Tumor volumes were recorded weekly. $^{**}P < 0.01$; $^{***}P < 0.001$. All experiments, except the xenograft tumor assay, were performed at least three times. Data are shown as mean ± standard deviations. *P* values were determined by Student's *t* test; $^{*}P< 0.05$, $^{**}P< 0.01$ and $^{***}P< 0.001$.

Supplementary Files

This is a list of supplementary files associated with this preprint. Click to download.

- SupplementaryFigureS1AC01.tif
- SupplementaryFigureS201.tif
- SupplementaryFigureS301.tif